†Electronic Supplementary Information (ESI)

Starvation induces diffusion hindrance at the nanoscale in mammalian cells.

Sakshi Sareen[1][a], Alicja Zgorzelska[a], Karina Kwapiszewska[a*], Robert Holyst[a*]

[a] Institute of Physical Chemistry, Polish Academy of Sciences, Warsaw, Poland

Sakshi Sareen
Soft Matter, Institute of Physical Chemistry, Polish Academy of Sciences, Warsaw, Poland

Alicja Zgorzelska
Soft Matter, Institute of Physical Chemistry, Polish Academy of Sciences, Warsaw, Poland

Karina Kwapiszewska
Soft Matter, Institute of Physical Chemistry, Polish Academy of Sciences, Warsaw, Poland

Robert Hołyst
Soft Matter, Institute of Physical Chemistry, Polish Academy of Sciences, Warsaw, Poland

Email address of corresponding authors:

Email: kkwapiszewska@ichf.edu.pl

Email: rholyst@ichf.edu.pl

Table of Contents

SI.1. Calculating diffusion coefficients of the probe in HeLa GFP cells

Confocal volume was calculated by obtaining the structural parameter (k) during the calibration step to measure diffusion coefficients.

$$\mathrm{D} = \frac{\omega_0^2}{4\tau_\mathrm{D}} \qquad \text{Eq.SI.1}$$

Where D is the diffusion coefficient [m^2/s], τ_D is diffusion time (s) obtained from FCS curve fitting of rhodamine 110 and ω_0 is the radius of the xy plane of focal volume (m).

$$\mathrm{r_h} = \frac{\mathrm{k_b T}}{6\pi \mathrm{ç D}} \qquad \text{Eq. SI.2}$$

Where k_b is the Boltzmann constant, T is the temperature (36˚C), and ç is the viscosity of water (Pa.s) at the given temperature.

For each experiment, the size of the confocal volume (V_{eff}) was calculated during calibration. According to the previously described protocol, FCS measurements were performed in 2.5 $\%_{wt}$ glucose in PBS buffer solution for Rhodamine 110 at 36°C (Kalwarczyk *et al., J. Phys. Chem. Lett*. 2017, 121, 9831). The diffusion coefficient of Rhodamine 110 in water at 25°C was previously measured using Pulsed Field Gradient–Nuclear Magnetic Resonance (Gendron et al., *J. Fluorescence*, 2008, 18, 1093). This value was used to calculate D in the reference medium (2.5$\%_{wt}$ glucose in PBS) at 36°C using the Stokes-Sutherland-Einstein equation and yielded a value of D = 560 µm^2/s. For our main experiments, effective nanoviscosity was calculated by obtaining the ratio of the diffusion coefficient of GFP molecule in the cell and the diffusion coefficient of GFP in water.

$$\frac{\mathrm{n_{eff}}}{\mathrm{n_0}} = \frac{\mathrm{D_0}}{\mathrm{D}} \qquad \text{Eq. SI.3}$$

Here, we define $H_{diff} = \frac{D_0}{D}$. Fluorescence intensity fluctuations of GFP molecules moving in and out of confocal volume as small as 0.2 - 0.5 fL. allows diffusion coefficient analysis in complex systems like cell cytoplasm. Single photon counting coupled with these measurements makes this technique highly sensitive to capture intensity fluctuations from nanoseconds to seconds on a time scale. We investigated changes in effective viscosity and H_{diff} in the cytoplasm under stressful conditions like starvation. GFP-transfected HeLa cells were used for these experiments. The GFP gene translates into GFP protein in the cell cytoplasm, which is ~28 kDa in size. Referring to the literature, the length and radii of GFP molecules are 4.2 nm and 2.4 nm, respectively[3]. The movement of these GFP molecules was recorded as a time trace, a function of intensity changes from ns and lasting 30 seconds per measurement. We obtained autocorrelation curves and used a one-component diffusion model to fit the data. When analyzed using quick fit and Python algorithm, these curves calculated the time of flight of GFP molecules. The LSDV model, defined by Holyst's group, measured the effective viscosity experienced by probes of different radii at different length scales ranging from 1-150 mm. Effective viscosity experienced by nano-objects was defined as nanoviscosity. Using Eq.SI.2,3, H_{diff} was calculated.

SI.2. FCS curves from H_{diff} measurements

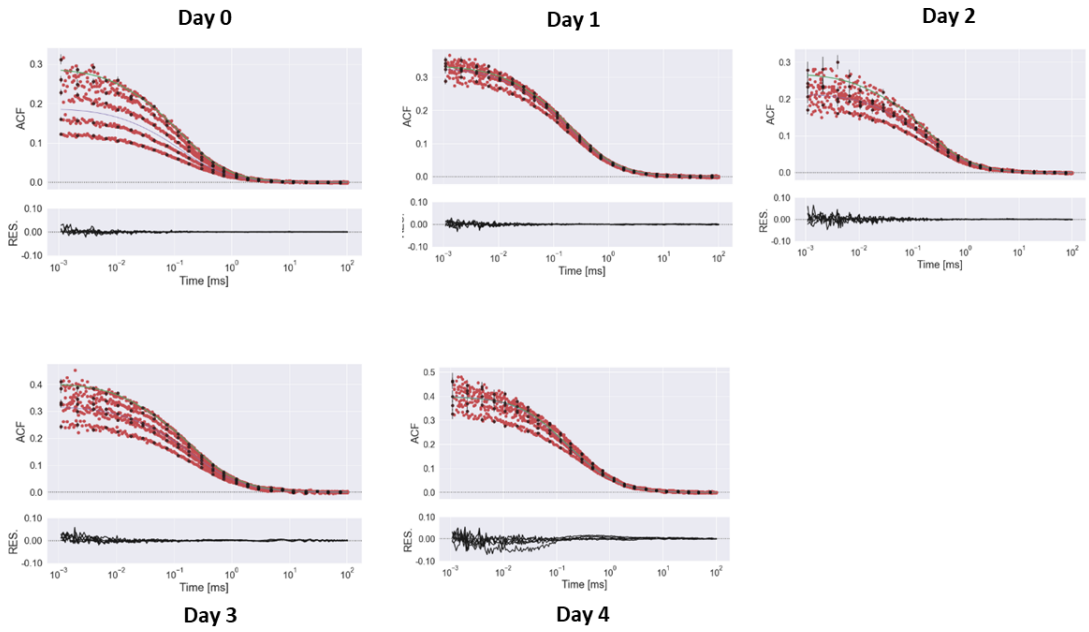

Fig SI.1: Autocorrelation curves of GFP molecules inside HeLa cells. Each graph (from left to right) represents 5 measurements taken per cell on different days of starving HeLa-GFP cells with. Each measurement was taken for 30 seconds with $\lambda_{ex} = 488\ \mathrm{nm}$ from cytoplasm. Here, fluorescence intensity has been calculated using one-component model and represented as a function of time. The data was analyzed using quick-fit software and python collectively.

SI.3 Relationship between GFP diffusion and cell volume

To describe effective nanoviscosity at different scales, we apply the length-scale dependent viscosity model (Eq. SI.4), which was previously proven valid in different human cell lines[4,5].

$$\eta_{eff} = \eta_0 A \exp\left[\left(\frac{\xi^2}{R_H{}^2} + \frac{\xi^2}{r_p{}^2}\right)^{\frac{-a}{2}}\right] \qquad \text{Eq. SI.4}$$

In the Eq. SI.4: η_{eff} stands for effective viscosity experienced by a probe of hydrodynamic radius r_p, η_0 is the viscosity of a solvent (water, 0.705 mPa·s for 36°C), A is a pre-exponential factor (equal to 1.3 ± 0.3 for HeLa cells), ξ is defined as an average half distance between major crowders (as explained in Fig SI.2, equal to 3.16 ± 0.14 nm for Hela cells[5]), R_H is an average hydrodynamic radius of major crowders (equal to 12.9 ± 2.3 nm for HeLa cells[5]), and a is an exponent defining liquid nanostructure[5] (equal to 0.62 ± 0.07 for HeLa cells[5]).

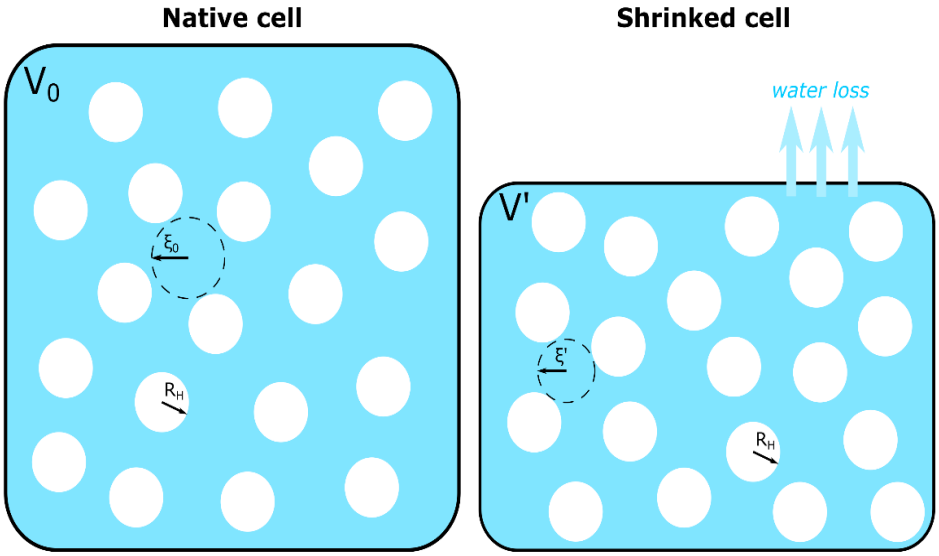

Fig SI.2: Schematic representation on how volume change can influence viscosity change in cells. Native cell (left panel), can be considered as a volume V_0 filled with crowders (white circles) of an average radii R_H. Size of the inter-crowder gaps can be described with ξ_0 parameter, which is an average half-distance between the crowders. Nanoviscosity or H_{diff} depends on both $\xi_{(0)}$ and R_H, as explained in Eq. S.I.4. When water loss occurs (right panel), the cell shrinks to volume V'. Number and size of crowders remains the same, while distances between the crowders reduces to ξ'. Reduction of ξ leads to H_{diff} (or nanoviscosity) increase, following Eq. S.I.4, 5.

Following the simple geometrical representation of cell shrinkage upon water efflux (Fig SI.2), the reduction of ξ parameter can be approximated with the formula Eq.SI.5:

$$\xi' = \xi_0 \sqrt[3]{\frac{V'}{V_0}} \qquad \text{Eq. SI.5}$$

Where initial values of V and ξ are indexed with "0", while values after cell shrinkage are indexed with " '". The effect of cell shrinkage on effective viscosity (η_{eff}) in HeLa cells is presented in Fig SI.3.

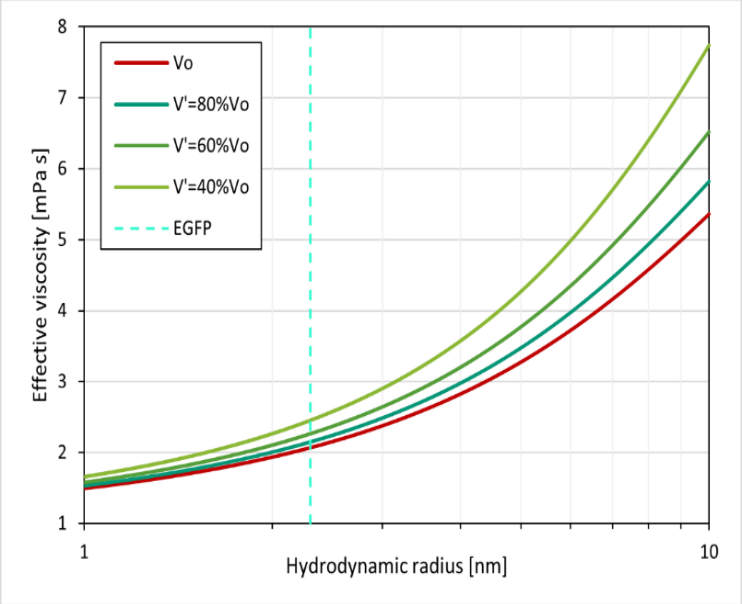

Fig SI.3: Changes of effective viscosity of cytoplasm of HeLa cells, calculated using Eq. SI.3, 4. Resulting volumes (V') are represented as % of initial volume (V_o), which led to changes in ξ' according to Eq.SI.5. Dashed line represents hydrodynamic radius of EGFP reported in this study.

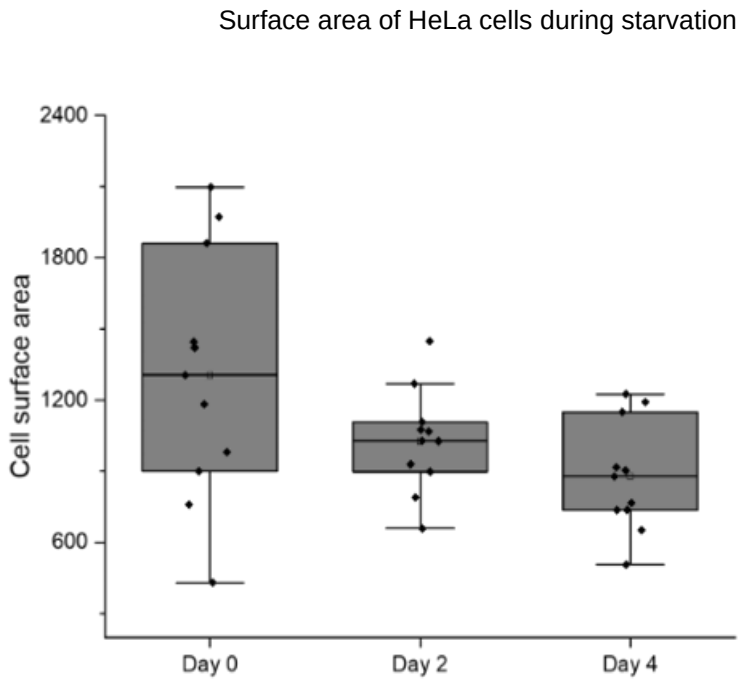

Fig SI.4: Surface area of starved cells. Cell surface area decreased over four days of cell starvation in HeLa GFP cells.

S.I.4 Interaction parameters between solvent and probe during starvation

Following K.Sozański et al.[6], the diffusion coefficient (D) in the crowded medium can be expressed as follows:

$$D = D_0 \exp\left[\frac{-E}{RT}\left(\frac{R_H}{\xi}\right)^a\right], \quad \text{Eq.SI.6}$$

Where D_0 is the diffusion coefficient in the pure solvent, R_H, ξ, and a are parameters derived from length-scale dependent viscosity model[1,5,7], and E is the interaction parameter, γ, for interactions between the probe and the crowders.

Upon cell stress, intermolecular spaces (ξ) decrease after water efflux occurs. Following the closer proximity of the molecules, a higher parameter γ is expected. Assuming detectable change in diffusion coefficients from D_1 (probe in control, native cells) to $D_{day0\text{-}4}$ (probe in a cell subjected to water efflux), γ parameter can be calculated as follows:

$$\ln\left(\frac{D_1}{D_0}\right) = \frac{-\gamma}{RT}\left(\frac{R_H}{\xi_1}\right)^a \quad \text{Eq.SI.7}$$

$$RT\left(\ln\left(\frac{D_1}{D_0}\right)\right) = -\gamma\left(\frac{R_H}{\xi_1}\right)^a$$

$$-\left[RT\left(\ln\left(\frac{D_1}{D_0}\right)\right)\left(\frac{R_H}{\xi_1}\right)^{-a}\right] = \gamma_1 \quad \text{Eq.SI.8}$$

γ_1 [kJ/mol] changes with changing diffusion coefficients and ξ (ξ_1 to ξ_2). Further, any change in overall activation energy is influenced by this parameter in complex fluid systems[8].

R_H – size parameter from length-scale dependent viscosity curve[4];
ξ_1 – size parameter from length-scale dependent viscosity curve[4];
**ξ_2 – size parameter calculated from volume change (from V_1 to V_2) experiment, following Eq. S.I.9:

$$\xi_2 = \xi_1 \sqrt[3]{\frac{V_2}{V_1}}, \quad \text{Eq. SI.9;}$$

a – exponent from length-scale dependent viscosity curve[4,5];
R – the gas constant;
T – temperature [K];
D_1 – diffusion coefficient of the probe measured in native cells;
D_0 – diffusion coefficient of the probe in water at temperature T.

Table SI.1. Comparison between relative diffusion and interaction parameter change for EGFP probe (2.3 nm)

Time of starvation	Calculated η/η0	Measured η/η0	D [um²/s]	ξ [nm]	γ [kJ/mol]
0 h	2.1	2.1	66.7	3.2	0.7
24h	2.2	2.5	50.5	2.0	0.7
48 h	2.2	2.6	43.3	2.8	1.1
72 h	2.3	3.2	33.5	2.6	1.2
96 h	2.3	4.5	31.7	2.5	1.3

Note: Calculated H_{diff} was obtained using LSDV, factoring in volume change.

SI.5 Fitting model for Yo-Pro-1 measurements

YO-PRO-1 dye is suspected to interact with tRNA, 40S rRNA, 60S rRNA, and 80S ribosomes. For target confirmation of YO-PRO-1, factors such as RNA mobility, brightness and abundance of individual RNA molecules were explored[1] in another study. Cells were stained with 50 nM YO-PRO-1 dye. Confocal images of cellular uptake of YO-PRO-1 in living cells were taken (Fig SI.5). Fixed cells stained with YO-PRO and DAPI were also imaged (Fig SI.5).

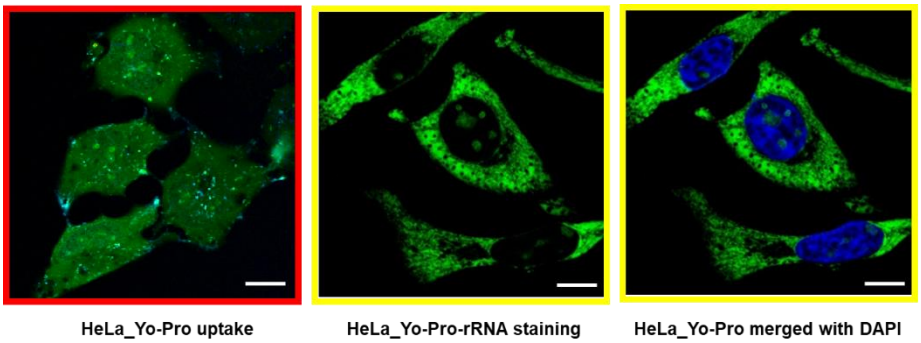

Fig SI.5: YO-PRO-1 uptake in HeLa cells. 50 nM YO-PRO-1 dye was taken up by living HeLa cells (far left in red). YO-PRO-1 staining of rRNA in fixed HeLa cell cytoplasm (middle in yellow). Counterstain DAPI (nucleus staining) was merged with YO-PRO-1 staining in fixed Hela cells (far right in yellow). YO-PRO-1 λ_{ex} = 488 nm and DAPI λ_{ex} = 405 nm. Scale bar: 20 µm.

FCS curves from Yo-Pro-1 stained cells were fitted with the following model[1]

$$G(\tau) = \left[q\left(\left\{ 1 + \left[fA_2 \exp\left(-\frac{6\tau k_B T}{8\pi\eta_R {r_{LSU}}^3} \right) \right] + \left[fA_4 \exp\left(-\frac{20\tau k_B T}{8\pi\eta_R {r_{LSU}}^3} \right) \right] \right\} \times \left\{ \frac{1}{N} \times \left[1 + \frac{2\tau k_B T}{3\pi\eta_T \omega_0^2 r_{LSU}} \right]^{-1} \times \left[1 + \frac{2\tau k_B T}{3\pi\eta_T \omega_0^2 \kappa^2 r_{LSU}} \right]^{-1/2} \right\} \right) + (1-q)\left(\left\{ \frac{1}{N} \times \left[1 + \frac{2\tau k_B T}{3\pi\eta_{T,tRNA} \omega_0^2 r_{tRNA}} \right]^{-1} \times \left[1 + \frac{2\tau k_B T}{3\pi\eta_{T,tRNA} \omega_0^2 \kappa^2 r_{tRNA}} \right]^{-1/2} \right\} \right) \right]$$

Eq. SI. 10

Details of the parameters of the above-described model are listed in Table SI.2. We reduced fitting parameters only to amplitudes (ratios between components) and viscosities sensed by the molecules. The rest of the parameters were fixed based on control experiments and theoretical models.

[1] *(Aneta Karpińska, Karolina Kucharska, Tomasz Kalwarczyk, Patrycja Haniewicz, Karina Kwapiszewska, Robert Hołyst "Measurement of large ribosomal subunit size in cytoplasm and nucleus of living human cells", Nanoscale Horizons, In Revision).*

Table SI.2. Parameters of the fitting model in SI.5

Parameter	Value		Fixed	Details
q	fitted		-	Relative fraction of 60S subunits to tRNA molecules, fitted in the range <0,1>
f	fitted		-	The amplitude of rotational diffusion
A_2	1,1071		✓	The amplitude of a rotational term, fixed for the value calculated based on [9]
A_4	0,0464		✓	The amplitude of a rotational term, fixed for the value calculated based on [9]
k_B	$1.38 \cdot 10^{-23}$ J/K		✓	Boltzmann constant
T	309.14 K		✓	Temperature set for the experiment.
r_{LSU}	15 nm		✓	Based on "Measurement of large ribosomal subunit size in cytoplasm and nucleus of living human cells" 2024, *submitted."*
η_R	varied		-	Effective viscosity for rotational diffusion of ribosomal 60S subunit, based on the models presented in [4,10]
η_T	varied		-	Effective viscosity for translational diffusion of ribosomal 60S subunit, based on the models presented in [4,10].
ω_0	~ 200 nm		✓	Size of the focal volume, determined during calibration preceding each experiment[1]
κ	~ 6		✓	The aspect ratio of the focal volume, determined during calibration preceding each experiment[1]
N	fitted		-	The average number of fluorescent molecules in the focal volume
r_{tRNA}	2 nm		✓	Hydrodynamic radius of tRNA molecules, determined experimentally in a buffer with FCS
$\eta_{T,tRNA}$	• 0.001936 Pa·s in cytoplasm • 0.00205 Pa·s in nucleus		-	Effective viscosity for translational diffusion of tRNA (r_p=2 nm), based on the models presented in [4,10]

Example fitting of the model with and without tRNA component to the data acquired in cytoplasm and nucleus is presented in Fig. SI.6 below:

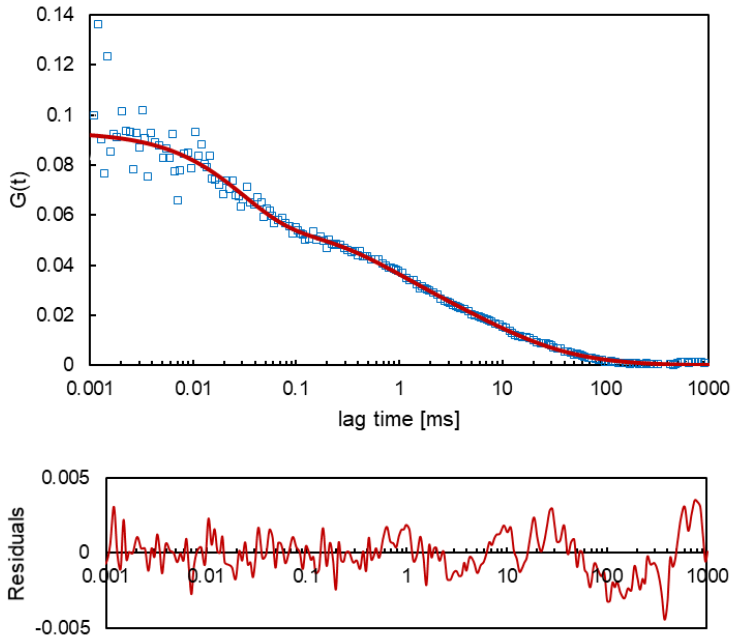

Fig SI.6: FCS curve from Yo-Pro-1 stained cytoplasm fitted with the model mentioned in S.I 5.

Translational diffusion of 40S ribosomes

Single-spot fluorescence acquisition in starved cells' cytoplasm resulted in extensive photobleaching of Yo-Pro-1 dye (Fig SI.7B). This pattern was different than in control cells (Fig SI.7A) and indicates the presence of immobilized molecules stained with Yo-Pro-1. After ~2 minutes of single-spot illumination, the fluorescence intensity signal stabilized (Fig SI.7C), and autocorrelation of fluorescence fluctuations was performed. Resulted FCS curves were fitted with the 2-component free-diffusion model (Fig SI.8). Obtained diffusion coefficients (~18 $\mu m^2/s$ at Day 1) were too high for a 15 nm molecule (60S) ribosome, which, together with the photobleaching phenomena, indicates immobilization of large ribosomal subunits in the starved cells. On the other hand, it could not be tRNA (2 nm), as its diffusion coefficient should be higher than for EGFP (2.3 nm, ~50 $\mu m^2/s$ at Day 1). Thus, we identified a freely diffusing object as a small ribosomal subunit (40S ribosome, 3.75 nm). FCS curves were obtained for Yo-Pro-1 stained 40S ribosomes in subsequent days, and a decreasing diffusion coefficient was observed with starvation (Fig SI.8).

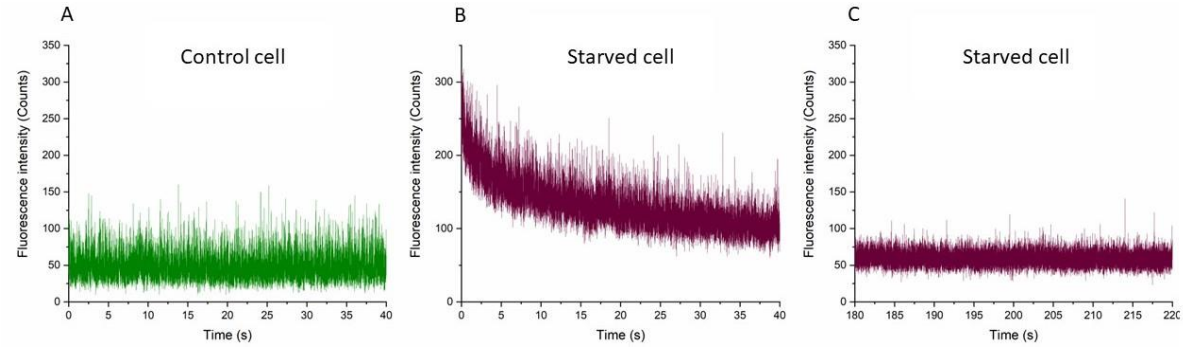

Fig SI.7: Fluorescence intensity in Yo-Pro-1 stained cells. A stable signal indicates freely diffusing objects, while photobleaching (B) indicates an immobile fraction of fluorescent molecules. (A) control cell (complete medium), (B) 96 h starved cell (0-40 seconds of measurement), (C) 96 h starved cell (the same cell, 180-220 seconds of measurement).

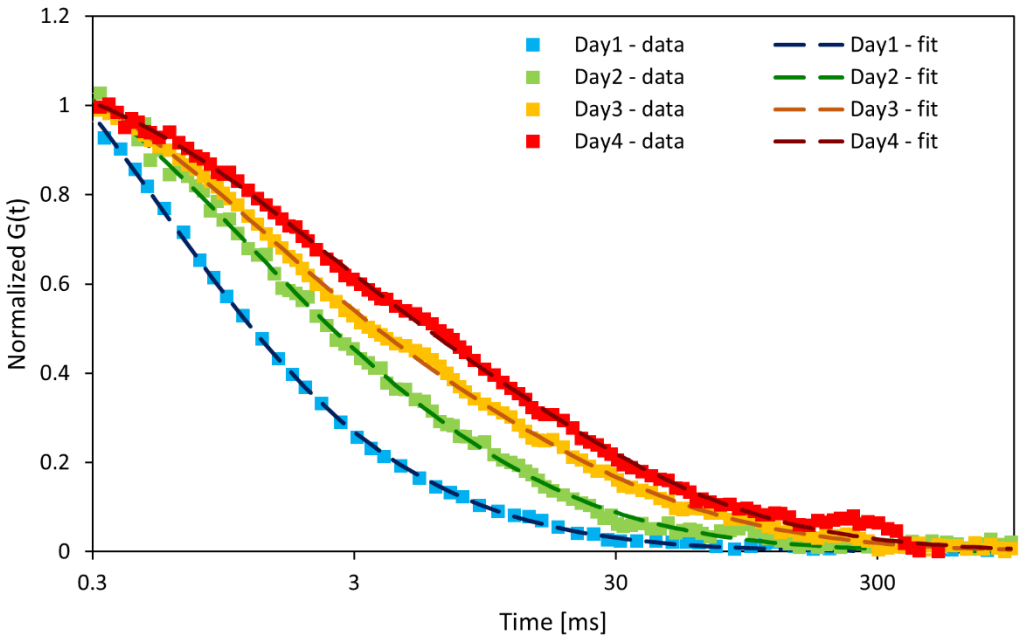

Fig SI.8: FCS curves of Yo-Pro-1 stained 40S ribosomes in the cytosol of starved HeLa cells. Curve shift towards longer diffusion times indicated increasing viscosity.

SI.6 Morphological changes during starvation

Starvation has profound effects on the physical properties of cells. Removing glucose alters the supply of the ultimate energy source, "ATP," and has been a topic of discussion among physicists and biologists equally[11]. In our study, we estimate the depletion of ATP during starvation using a genetic nanosensor. 769-P cells were transfected with MalionR (transfection efficiency of 769-P cells with MALIONR genetic nanosensor, using lipofectamine, was found to be most agreeable for confocal imaging experiments, which is why this cell line was used to conduct cell morphology studies in starvation conditions) which produces a subunit of F_0-F_1 ATP synthase is responsible for binding to ATP and fluoresce. The fluorescence changes in cells cultured in glucose-deprived phosphate saline buffer, containing only calcium and magnesium ions[12], were monitored. 769-p cells are renal carcinoma cells, widely used in studies associated with cancer metabolism. Since kidney cells are one of the largest consumers of glucose, experiments were thus performed to study the morphological changes in glucose-depleted conditions (prolonged starvation) in these cells during reducing ATP concentrations. 769-P cells were kept in a nutrient-deprived buffer (PBS) for 120 hours. Confocal microscopy revealed a decrease in fluorescence intensity after approximately 22 hours of starvation. This highlights the reliance of cancer cells on external energy sources for their maintenance. A small population of cells detached from the surface of the glass bottom dish around 20 hours of starvation. Further growth rate increase was limited after 21 hours compared to control cells in regular cell culture media. No noticeable morphological changes were recorded in 769-P cells till 19 hours of starvation in PBS. Noticeable reduction in ATP levels was observed till 30 hours (deduced from confocal image analysis, Fig SI.9). However, significant morphological alterations occurred after 40 hours, marked by the formation of macropinocytotic cups (Fig SI.9; red star) overlapping with breakage of cell-cell contacts (Fig SI.9; yellow arrow). These cups expanded and contracted, displaying enhanced motility in media over time. By 48 hours, finger-like projections were evident under the confocal microscope, persisting until the end of measurements. Membrane blebbing started after 72 hours of starvation, and after 90 hours, 90% of cells became circular and motile, with continued finger-like projections (Fig SI.9; green circle). Control cells in media remained attached[13].

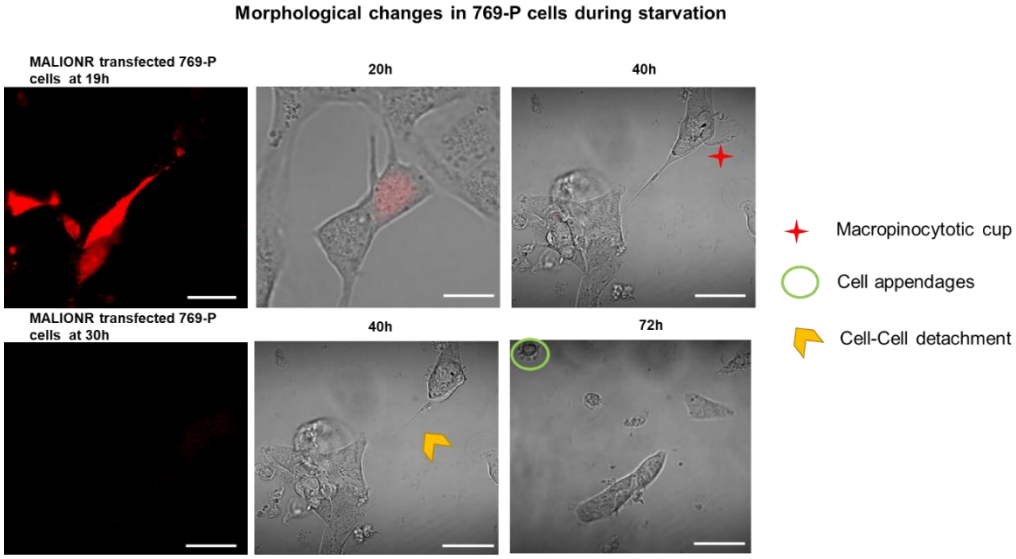

Fig SI.9: Confocal images of 769-P cells at 60X. 769-P cells transfected with MALIONR plasmid containing gene sequence of ATP synthase protein where, F_0F_1-ATP synthase protein fluoresces after binding with intracellular ATP. Cells were imaged for 96 hours in phosphate saline buffer (without glucose and other cell nutrients). ATP-dependent fluorescence is reduced drastically by the end of 30 hours. 40 hours after starvation, a macropinocytotic cup could be seen (red star). The cell-cell attachment was broken after 40 hours of starvation (yellow arrow). Cell appendages could be seen around 72 hours of starvation (green circle). These appendages helped in increased cell motility. Scale bar: 60 µm.

SI.7 MTT assay for cell viability during starvation

We performed an MTT assay on HeLa cells kept in PBS for 4 days, seeded at different cell densities/wells (Fig SI.10). This assay measured the overall cellular stress as the effect of prolonged starvation. % viability was calculated on day 4 for cells cultured in PBS and whole growth media using the formulae below:

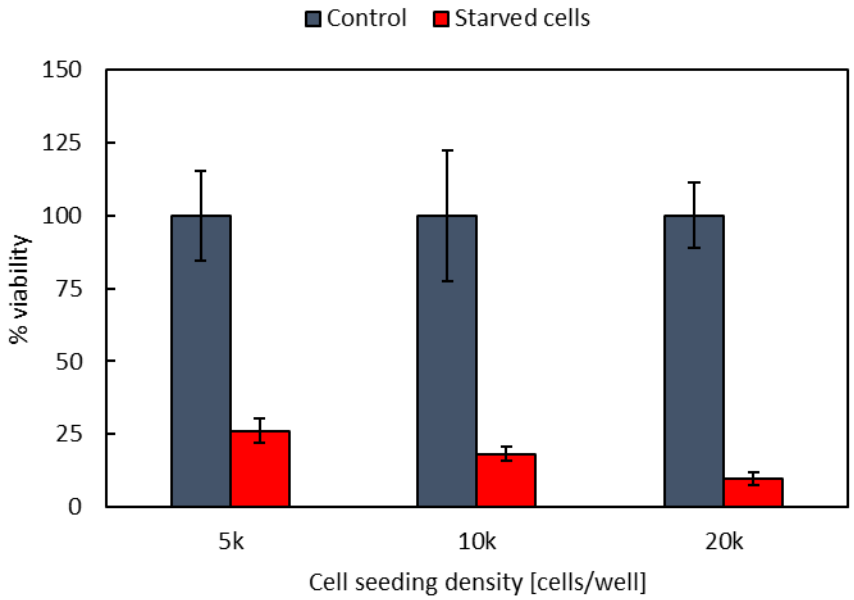

Fig SI.10: Cell viability assay using MTT on HeLa cells during prolonged starvation. The measurements were averaged (for each seeding density) from 8-10 wells from a 96-well plate.

Notably, the reduced % viability in this experiment is the result of three factors: (1) cell death, (2) stopping of proliferation, and (3) reduced metabolic activity of the remaining cells.

SI.8 Confocal volume positioning for FCS

FLIM images were recorded beforehand on a confocal microscope for FCS measurement in the cytoplasm and nucleus. These images determined the position of confocal volume inside cells in different compartments. While focusing the objective on the cells, it was observed that the fluorescent signal decreased both – when the objective was moving closer to the cell (attached to the glass surface; Fig SI.11, image 1) and moving further into the slide (above the cell; Fig SI.11, image 2). Therefore, the confocal volume was placed in the middle of these positions on the z-axis, where the central part of the cell (lighter) was the nucleus, and everything around it (denser) was considered as cell cytoplasm (Fig SI.11, image 3). Nucleoli or denser membrane structures (like ER in the cytoplasm) were avoided by recording distinct measurements from different areas in cells.

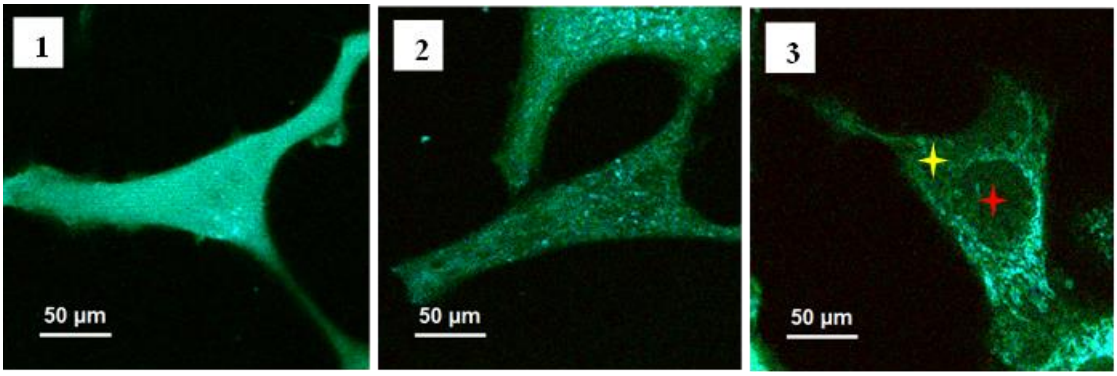

Fig SI.11: FLIM images showing the positioning of confocal volume inside cell nucleus and cytoplasm for FCS measurements

References:

1. Kalwarczyk, T. *et al.* Apparent Anomalous Diffusion in the Cytoplasm of Human Cells: The Effect of Probes' Polydispersity. *Journal of Physical Chemistry B* 2017, **121**, 9831–9837.
2. Gendron, P.-O., Avaltroni, F. & Wilkinson, K. J. Diffusion Coefficients of Several Rhodamine Derivatives as Determined by Pulsed Field Gradient–Nuclear Magnetic Resonance and Fluorescence Correlation Spectroscopy. *J Fluoresc* 2008, **18**, 1093–1101.
3. Hink, M. A. *et al.* Structural dynamics of green fluorescent protein alone and fused with a single chain Fv protein. *Journal of Biological Chemistry* 2000, **275**, 17556–17560.
4. Kwapiszewska, K. *et al.* Determination of oligomerization state of Drp1 protein in living cells at nanomolar concentrations. *Sci Rep* 2019, **9**, 1–9.
5. Kwapiszewska, K. *et al.* Nanoscale Viscosity of Cytoplasm Is Conserved in Human Cell Lines. *Journal of Physical Chemistry Letters* 2020, **11**, 6914–6920.
6. Sozański, K., Wiśniewska, A., Kalwarczyk, T. & Hołyst, R. Activation energy for mobility of dyes and proteins in polymer solutions: From diffusion of single particles to macroscale flow. *Phys Rev Lett* 2013, **111**, 1–5.
7. Kalwarczyk, T. *et al.* Comparative Analysis of Viscosity of Complex Liquids and Cytoplasm of Mammalian Cells at the Nanoscale. *Nano Lett* 2011, **11**, 2157–2163.
8. Agasty, A., Wisniewska, A., Kalwarczyk, T., Koynov, K. & Holyst, R. Macroscopic Viscosity of Polymer Solutions from the Nanoscale Analysis. *ACS Appl Polym Mater* 2021, **3**, 2813–2822.
9. Aragón, S. R. & Pecora, R. Fluorescence correlation spectroscopy and Brownian rotational diffusion. *Biopolymers* 1975, **14**, 119–137.
10. Bubak, G. *et al.* Quantifying Nanoscale Viscosity and Structures of Living Cells Nucleus from Mobility Measurements. *Journal of Physical Chemistry Letters* 2021, **12**, 294–301.
11. Mookerjee, S. A., Gerencser, A. A., Nicholls, D. G. & Brand, M. D. Quantifying intracellular rates of glycolytic and oxidative ATP production and consumption using extracellular flux measurements. *Journal of Biological Chemistry* 2017, **292**, 7189–7207.
12. Young Hee Choi, and A.-M. Y., HHS Public Access. *Physiol Behav* 2019, **176**, 139–148.
13. Chiodi, I., Picco, G., Martino, C. & Mondello, C. Cellular response to glutamine and/or glucose deprivation in in vitro transformed human fibroblasts. *Oncol Rep* 2019, **41**, 3555–3564.